

# Consequences of neutron-proton pairing correlations for the rotational motion of the $N=Z$ nucleus $^{72}\text{Kr}$

N. S. Kelsall,<sup>1</sup> R. Wadsworth,<sup>1</sup> A. N. Wilson,<sup>1,\*</sup> P. Fallon,<sup>2</sup> A. O. Macchiavelli,<sup>2</sup> R. M. Clark,<sup>2</sup> D. G. Sarantites,<sup>3</sup> D. Seweryniak,<sup>4</sup> C. E. Svensson,<sup>2,†</sup> S. M. Vincent,<sup>5,‡</sup> S. Frauendorf,<sup>5,6</sup> J. A. Sheikh,<sup>7</sup> and G. C. Ball<sup>8</sup>

<sup>1</sup>*Department of Physics, University of York, Heslington, York YO10 5DD, United Kingdom*

<sup>2</sup>*Nuclear Science Division, Lawrence Berkeley National Laboratory, Berkeley, California 94720*

<sup>3</sup>*Department of Chemistry, Washington University, St. Louis, Missouri 63130*

<sup>4</sup>*Physics Division, Argonne National Laboratory, Argonne, Illinois 60439*

<sup>5</sup>*Department of Physics, University of Notre Dame, Notre Dame, Indiana 46556*

<sup>6</sup>*IKHP, Research Center Rossendorf, PF 510119, D-01314 Dresden, Germany*

<sup>7</sup>*Physik-Department, Technische Universität München, D-85747 Garching, Germany*

<sup>8</sup>*TRIUMF, 4004 Wesbrook Mall, Vancouver, British Columbia, Canada V6T 2A3*

(Received 15 March 2001; published 9 July 2001)

High-spin states in the  $N=Z$  nucleus  $^{72}\text{Kr}$  were populated using the  $^{40}\text{Ca}(^{36}\text{Ar},2p2n)$  reaction at a beam energy of 145 MeV. The yrast band has been observed up to a tentative spin of  $20\hbar$ . Nonyrast rotational structures have also been observed for the first time. The alignment of  $g_{9/2}$  protons and neutrons in the yrast band is observed to be significantly delayed relative to the heavier even-even Kr isotopes. Exact deformed cranked shell model calculations suggest that this could be due to the combined effect of isovector ( $T=1$ ) and isoscalar ( $T=0$ ) neutron-proton pairing correlations.

DOI: 10.1103/PhysRevC.64.024309

PACS number(s): 21.10.Re, 21.60.-n, 23.20.Lv, 27.50.+e

## I. INTRODUCTION

$N=Z$  nuclei are of special interest because identical single particle orbitals are available to both protons and neutrons. The simultaneous filling of orbitals is predicted to result in a significant enhancement of neutron-proton ( $np$ ) pairing correlations [1] with respect to the more established like-nucleon ( $nn$  and  $pp$ ) pairing modes. In like-nucleon pairing, the nucleons are constrained by the Pauli exclusion principle so that they can only form  $J=0, T=1$  (isovector) pairs. However, for  $np$  pairing this constraint is removed and the nucleons can also couple together to form  $J=1, T=0$  (isoscalar) pairs. The existence and properties of these isoscalar and isovector modes of  $np$  pairing in  $N\sim Z$  nuclei have been the subject of a recent revival of theoretical interest (e.g., see Refs. [2,3]).

The existence of full ( $nn, pp, np$ )  $T=1$  pairing correlations is confirmed by an analysis of binding energy differences along the  $N=Z$  line [4,5]. However, these same data, together with an analysis of pairing phonons near  $^{40}\text{Ca}$  and  $^{56}\text{Ni}$  [6,7], suggest that there is not a coexisting condensate of deuteron like ( $T=0$ )  $np$  pairs. While these data appear to rule out strong isoscalar pairing correlations in the ground state, it is still possible that they may play an important role

at higher spins. This is the subject of the present work.

A predicted spectroscopic signature of  $T=0$  pairing correlations at high spins in even-even  $N=Z$  nuclei is a delay of the crossing frequency between the four quasiparticle band, containing aligned neutrons and protons, and the vacuum configuration, compared to that in heavier even-even isotopes. For a single- $j$  shell, both shell model [2] and cranked Hartree-Fock [8,9] calculations suggest that the delay in the crossing frequency may be attributed to isovector  $np$  pairing correlations alone. However, the work by Sheikh and Wyss [9] also suggests that for realistic cases in heavy nuclei ( $Z > 28$ ) with several  $j$  shells, the  $J=1$  component of the isoscalar pairing field may acquire a substantial strength. This would result in significant changes to the band crossing frequencies for  $N=Z$  nuclei.

A delay in the alignment frequency of pairs of  $g_{9/2}$  protons and neutrons in the yrast band of  $^{72}\text{Kr}$ , relative to the heavier  $^{74,76}\text{Kr}$  isotopes, was initially reported by de Angelis *et al.* [10] as possible evidence for the  $np$  pairing mode. The backbend reported by these authors was first shown to be incorrect by Hausladen [11] and more recently by Fischer and Lister [12]. The latter work did, however, show that there is a significant delay in the  $g_{9/2}$  proton and neutron crossing frequencies. The present work, which was carried out in parallel with that of Ref. [12], confirms that the backbend does not exist in the yrast band and that there is a substantial delay in crossing frequency, which is marked by a gradual upbend in the moment of inertia. Our results are compared with cranking calculations within a single- $j$  shell ( $g_{9/2}$ ) that include  $np$  pairing. These suggest that both isoscalar and isovector components could play an important role in delaying the crossing frequency; however, the existence of an oblate shape at high spin could also explain the observed data.

\*Present address: Department of Nuclear Physics, Australian National University, Canberra ACT 0200, Australia.

†Present address: Department of Physics, University of Guelph, Guelph, Ontario, Canada N1G 2W1.

‡Present address: Physics Department, University of Surrey, Guildford, Surrey GU2 7XH, UK.

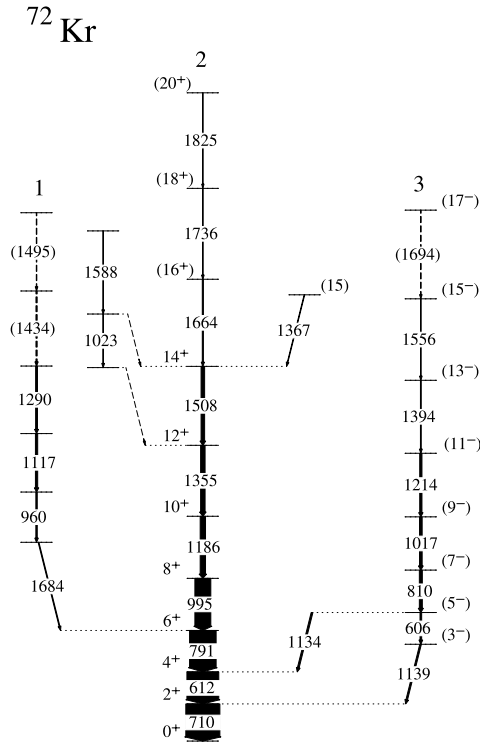


FIG. 1. Proposed level scheme for  $^{72}\text{Kr}$  deduced from the present work.

## II. EXPERIMENTAL DETAILS AND DATA ANALYSIS

High-spin states in  $^{72}\text{Kr}$  were produced via the  $^{40}\text{Ca}(^{36}\text{Ar}, 2p2n)$  reaction at a beam energy of 145 MeV. The beam was incident upon a target consisting of a  $390\text{ }\mu\text{g}/\text{cm}^2$  thick  $^{40}\text{Ca}$  foil with  $113\text{ }\mu\text{g}/\text{cm}^2$  and  $97\text{ }\mu\text{g}/\text{cm}^2$  flashes of Au in front and behind, respectively, to prevent oxidization of the Ca foil. Emitted  $\gamma$  rays were detected using the Gammasphere array [13] which consisted of 78 escape suppressed HPGe detectors. Due to the small cross section for the production of  $^{72}\text{Kr}$  a highly efficient method of channel selection was necessary in order to identify the  $\gamma$  rays associated with this nucleus from the many other more favored reaction channels. To achieve this, charged particles and neutrons were detected using the Microball array [14] and the neutron shell [15], respectively. The latter consists of 30 tapered hexagonal BC-501A scintillator detectors which replaced 30 suppressed Ge detectors at the forward most angles of Gammasphere. Data were collected using a trigger containing either at least two suppressed Ge detectors firing in coincidence with one or more neutrons being detected in the neutron shell or greater than four suppressed Ge detectors firing in prompt coincidence. Approximately  $8 \times 10^8$  events were written to tape.

Effects of particle evaporation upon the recoiling nucleus were compensated for by using information from the Microball to perform a full kinematic reconstruction [16]. Data were sorted offline into an  $E_\gamma$ - $E_\gamma$  matrix and an  $E_\gamma$ - $E_\gamma$ - $E_\gamma$  cube, both with particle gates of one or two protons, zero alpha particles, and at least one neutron in order to enhance the  $^{72}\text{Kr}$  reaction channel. These were then analyzed using the RADWARE suite of software packages [17]. A direc-

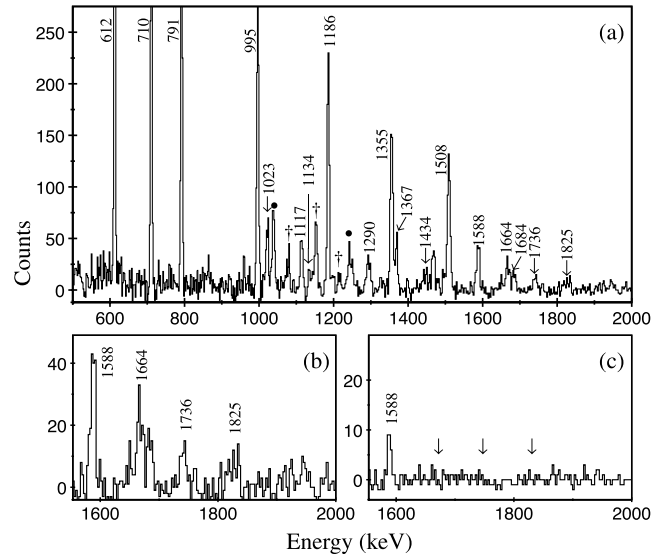


FIG. 2. (a) Gated coincidence spectrum showing the yrast band in  $^{72}\text{Kr}$  created from a sum of doubles gates in a RADWARE cube. All yrast transitions up to the  $14^+$  level were included in the gate list. Peaks marked with a  $\dagger$  or  $\bullet$  are contaminants from  $^{73}\text{Kr}$  and  $^{72}\text{Br}$ , respectively. (b) shows an expansion of (a). (c) shows a gated coincidence spectrum created from a sum of doubles gates which included all transitions in the yrast band up to the  $12^+$  level against the 1023 keV  $\gamma$  ray. The arrows indicate the positions of the 1664, 1736, and 1825 keV  $\gamma$  rays. All energies are labeled in keV.

tional correlation from oriented states (DCO) [18]  $E_\gamma - E_\gamma$  matrix was also sorted for the purpose of extracting the multipolarities of the transitions. The DCO matrix was constructed using detectors from the  $79^\circ$  to  $101^\circ$  rings on the  $x$  axis and all other detectors being used to increment the  $y$  axis. This was done using the same particle gates as discussed above. DCO ratios for known stretched quadrupole  $\leftrightarrow$  stretched quadrupole and stretched quadrupole  $\leftrightarrow$  stretched dipole transitions were found to be 1.1 and 0.8, respectively.

### III. RESULTS

Analysis of the present data enabled the level scheme shown in Fig. 1 to be constructed for  $^{72}\text{Kr}$ . We have been able to observe the yrast band up to a tentative spin of  $20\hbar$ . The observed yrast sequence is consistent with that deduced by Fischer and Lister [12]. It would appear, however, that the  $2p2n$  exit channel does not populate as high in spin as the  $2\alpha$  channel, which was used in their work, since they were able to observe states up to a tentative spin of  $26\hbar$ . The spectrum shown in Fig. 2(a) was produced via a sum of double gates from the cube as detailed in the figure caption. It was only possible to extract DCO ratios for a few of the transitions (see Table I) due to a lack of statistics and contamination. These suggest that the transitions within the yrast band (band 2) up to the  $14^+$  level are quadrupole in nature, consequently these have been assigned as  $E2$  transitions. The work of de Angelis *et al.* [10] placed a 1367 keV  $\gamma$  ray directly on top of the 1508 keV transition in the yrast band. The present work supports the existence of the transition and

TABLE I. Intensities,  $\gamma$ -ray energies, and DCO ratios for transitions in  $^{72}\text{Kr}$  from the present work.

$E_\gamma$ (keV)	$I_{rel}(\%)$	DCO	Multipolarity	$I_i^\pi(\hbar)$	$I_f^\pi(\hbar)$
606(8)	5(1)		(E2)	(5 <sup>-</sup> )	(3 <sup>-</sup> )
611.6(1)	93(12)	$0.97^{+0.08}_{-0.07}$	E2	4 <sup>+</sup>	2 <sup>+</sup>
709.7(1)	100(8)	$1.25^{+0.15}_{-0.13}$	E2	2 <sup>+</sup>	0 <sup>+</sup>
791.5(1)	78(9)	$1.34^{+0.14}_{-0.12}$	E2	6 <sup>+</sup>	4 <sup>+</sup>
810(3)	9(2)		(E2)	(7 <sup>-</sup> )	(5 <sup>-</sup> )
960.0(3)	4(1)				
995.5(1)	47(8)	$0.97^{+0.10}_{-0.09}$	E2	8 <sup>+</sup>	6 <sup>+</sup>
1017.2(8)	8(3)		(E2)	(9 <sup>-</sup> )	(7 <sup>-</sup> )
1023(1)	2(2)				
1117(2)	7(1)				
1134.1(1)	5(1)	$0.84^{+0.17}_{-0.14}$	(E1)	(5 <sup>-</sup> )	4 <sup>+</sup>
1139.3(2)	5(2)		(E1)	(3 <sup>-</sup> )	2 <sup>+</sup>
1185.9(8)	16(4)	$0.95^{+0.12}_{-0.10}$	E2	10 <sup>+</sup>	8 <sup>+</sup>
1214.3(5)	6(2)		(E2)	(11 <sup>-</sup> )	(9 <sup>-</sup> )
1290(1)	5(3)				
1355.1(1)	13(7)	$1.18^{+0.18}_{-0.16}$	E2	12 <sup>+</sup>	10 <sup>+</sup>
1367(8)	1.7(4)	$0.67^{+0.19}_{-0.15}$	(M1/E1)	(15)	14 <sup>+</sup>
1394(1)	2.3(8)		(E2)	(13 <sup>-</sup> )	(11 <sup>-</sup> )
1434(2)	4(2)				
1495(1)	1.4(7)				
1508.1(3)	10(3)	$1.12^{+0.19}_{-0.16}$	E2	14 <sup>+</sup>	12 <sup>+</sup>
1556(4)	1.5(1)		(E2)	(15 <sup>-</sup> )	(13 <sup>-</sup> )
1588(1)	1.7(2)				
1664.2(4)	3.2(2)		(E2)	(16 <sup>+</sup> )	14 <sup>+</sup>
1683.9(9)	2.3(7)				6 <sup>+</sup>
1694(4)	1.3(8)		(E2)	(17 <sup>-</sup> )	(15 <sup>-</sup> )
1736.0(6)	1.5(2)		(E2)	(18 <sup>+</sup> )	(16 <sup>+</sup> )
1825(20)	1(1)		(E2)	(20 <sup>+</sup> )	(18 <sup>+</sup> )

its placement within the decay scheme, however, the DCO value for this  $\gamma$  ray suggests that the radiation is dipole in nature (see Table I). From the present work there is no evidence for any additional  $\gamma$  rays in this sequence, which may suggest that the 1367 keV transition comes from a favored terminating state.

Figure 2(b) highlights the high energy transitions in the upper portion of the spectrum shown in Fig. 2(a). Figure 2(c) shows that the 1588 keV  $\gamma$  ray also appears to result from the decay of a favored terminating state since there is once again no evidence of a rotational-like  $\gamma$  cascade in the spectrum either above (or below) this transition. This  $\gamma$  ray is in coincidence with the 1508 keV  $\gamma$  ray and it is possible that it directly feeds the 14<sup>+</sup> state. The 1023 keV  $\gamma$  ray is not in coincidence with the 1508 keV transition [see Fig. 3(d)], but is in coincidence with the 1355 and 1588 keV transitions. However, because we were unable to find evidence for a transition linking the 1023 keV  $\gamma$  ray back into the yrast sequence at the 12<sup>+</sup> state we have shown the 1023 and 1588 keV transitions with tentative links into the decay scheme. Clearly, if the 1588 keV transition does decay directly to the 14<sup>+</sup> state, and it is an E2 transition, then this would be very interesting since it would be the yrast 16<sup>+</sup> state.

The absence of any other transitions feeding the 14<sup>+</sup> state, other than the ones already discussed, leads us to conclude (in agreement with Fischer and Lister [12]) that the 1664, 1736, and 1825 keV  $\gamma$  rays form the continuation of the yrast band. The large decrease in intensity observed in Fig. 2(a) for these transitions compared to those from states below the 14<sup>+</sup> level results from the fact that the 1367 and 1588 keV  $\gamma$  rays, which also feed the 14<sup>+</sup> state, have similar intensities to the 1664 keV  $\gamma$  ray. It was not possible to extract DCO ratios for most of the transitions above the 1508 keV  $\gamma$  ray, hence in the following discussion the yrast band transitions have been assumed to have E2 multipolarity.

Two new rotational structures (bands 1 and 3 in Fig. 1) have been observed for the first time in this work. Figures 3(a) and 3(b) show spectra illustrating the transitions in bands 1 and 3, respectively. The 791 keV transition in Fig. 3(b) is a contaminant. This is confirmed by Fig. 3(c), where the spectrum has been generated from the cube using gates on the 606 and 612 keV  $\gamma$  rays in coincidence with the 810, 1017, 1214, and 1394 keV transitions. The 791 keV  $\gamma$  ray is clearly absent in this spectrum, indicating that its presence in Fig. 3(b) results from contamination.

It is clear from the statistics in the above spectra that the

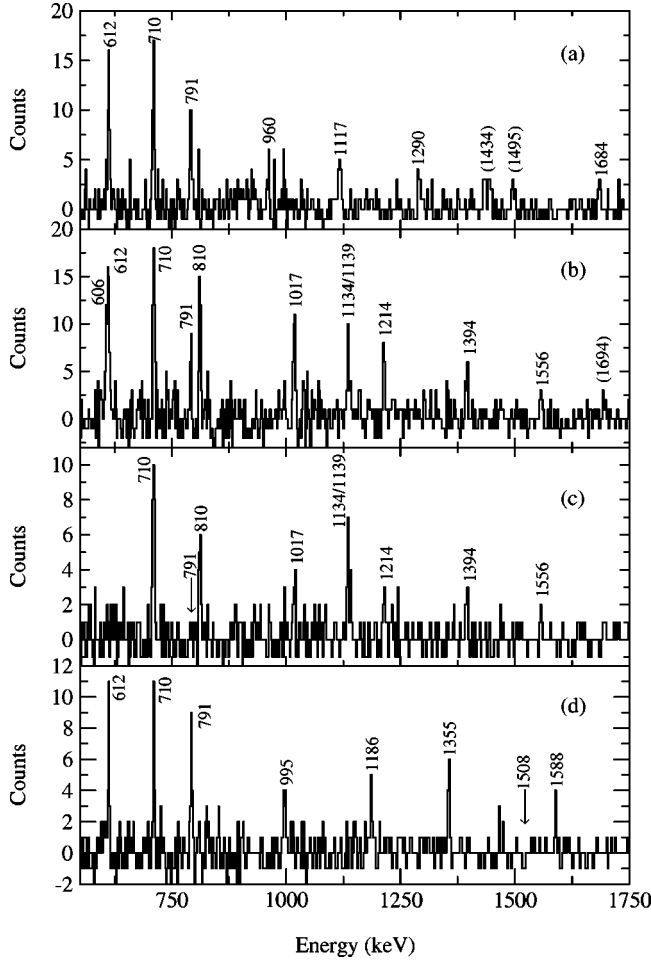


FIG. 3. (a) Coincidence spectrum from the particle gated cube showing band 1. The spectrum was created by taking the bottom three transitions from the yrast band (710, 612, and 791 keV) in coincidence with 1684, 960, 1117, and 1290 keV transitions from band 1. (b) Spectrum showing the transitions in band 3. The spectrum was created by taking the 710, 612, 1134, and 1139 keV  $\gamma$  rays in coincidence with the lowest five transitions from band 3 (606, 810, 1017, 1214, and 1394 keV). (c) shows a spectrum created using gates on the 612 and 606 keV  $\gamma$  rays in coincidence with the 810, 1017, 1214, and 1394 keV  $\gamma$  rays from band 3. Note the absence of the 791 keV  $\gamma$  ray. (d) This spectrum was created by taking the 1023 keV transition in coincidence with all  $\gamma$  rays in the yrast band up to the 1355 keV transition, the missing 1508 keV  $\gamma$  ray is indicated with an arrow. In all cases  $\gamma$ -ray energies are marked in keV.

bands are very weakly populated. As a result, it was only possible to obtain DCO information for one transition (1134 keV) linking band 3 to band 2. The DCO ratio for the 1134 keV  $\gamma$  ray was obtained from the relevant matrix using a gate on the 612 keV transition, thereby avoiding contamination from the 1139 keV transition. These data together with systematics from the even Kr isotopes (e.g., in  $^{74}\text{Kr}$  [19] two odd spin and one even spin negative parity bands are observed to decay into the yrast  $4^+$  state) tentatively suggests that the states within band 3 have odd spin and negative parity. If the transitions from band 3 to band 1 are indeed of  $E1$  character then this would clearly be interesting since for

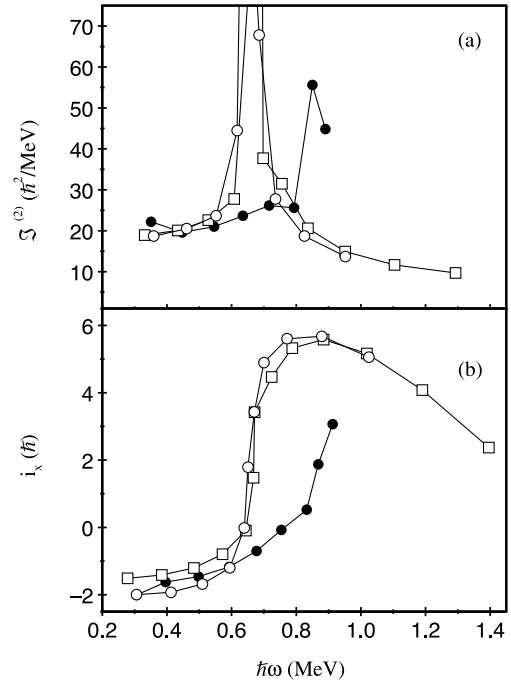


FIG. 4. (a) The dynamic moments of inertia  $\mathcal{J}^{(2)}$  for the yrast bands in  $^{72,74,76}\text{Kr}$  as a function of rotational frequency. (b) The alignment  $i_x$  for the yrast bands in  $^{72,74,76}\text{Kr}$  (the Harris parameters used were  $\mathcal{J}_0 = 18$ ,  $\mathcal{J}_1 = 0$ ). Filled circles represent the experimental data points for  $^{72}\text{Kr}$  while the open squares and circles show the points for  $^{74,76}\text{Kr}$ , respectively.

$N=Z$  nuclei the matrix elements of the isovector  $E1$  operator should vanish if the initial and final states have the same isospin. However, since the spins and parities of the two side bands (bands 1 and 3) are uncertain, they will not be discussed further. In this paper we wish to focus upon the properties of the yrast band structure of  $^{72}\text{Kr}$ .

#### IV. DISCUSSION

The dynamic moments of inertia for the yrast bands in the three even-even  $^{72,74,76}\text{Kr}$  isotopes are shown in Fig. 4(a). Figure 4(b) shows the alignment plots for the same nuclei. Both figures clearly indicate that there is a substantial delay in the frequency at which the alignment of pairs of  $g_{9/2}$  protons and neutrons occurs in  $^{72}\text{Kr}$  ( $\sim 0.85$  MeV/ $\hbar$ ) compared to the crossing frequency observed in  $^{74,76}\text{Kr}$  ( $\sim 0.65$  MeV/ $\hbar$ ). Furthermore, it is interesting to note that the observed alignment gain in  $^{74,76}\text{Kr}$  ( $\sim 7.5\hbar$ ) is somewhat lower than cranking calculations predict for the alignment of pairs of  $g_{9/2}$  neutrons and protons ( $\sim 13\text{--}15\hbar$ ) in these nuclei. This aspect will be discussed further below.

Previous work on  $^{72}\text{Kr}$  [10] suggests that there is an oblate  $\rightarrow$  prolate shape transition at low spin ( $\sim 4\text{--}6\hbar$ ), with the quadrupole deformation of the nucleus being  $\sim 0.4$  prior to the alignment of the  $g_{9/2}$  protons and neutrons. This shape transition is further supported by recent calculations based on the excited Vampir variational approach [20]. Standard cranked shell model (CSM) calculations [21] for this nucleus, with deformation parameters  $\beta_2 = 0.4$ ,  $\gamma = 0^\circ$ , pre-



dict that the  $g_{9/2}$  proton and neutron crossing frequencies occur at  $\sim 0.56$  MeV/ $\hbar$ . This is much less than the experimentally observed value. If the nucleus is prolate or triaxial ( $\gamma = -30^\circ$ ) then the deformation would have to be increased to an unrealistically large value ( $\beta_2 \geq 0.6$ ) in order to reproduce the observed crossing frequencies. Similar calculations for the  $T_z = 1$  nucleus  $^{74}\text{Kr}$  yield essentially the same crossing frequencies for the protons (0.55 MeV/ $\hbar$ ) and neutrons (0.57 MeV/ $\hbar$ ). These values are also somewhat lower than the experimentally observed values, indicating that standard CSM calculations for a prolate or moderately triaxial shape cannot describe the properties of these nuclei at high spin.

For an oblate deformation of 0.4, however, CSM calculations predict that the  $g_{9/2}$  protons and neutrons align at a frequency of  $\sim 0.8$  MeV/ $\hbar$ , in good agreement with the experimental data. The possibility that the shift in frequency may be due to a substantially different shape of the neighboring isotopes was considered in Ref. [10]. Calculations were performed for the  $^{72,74,76}\text{Kr}$  nuclei using the new pairing and deformation self-consistent total Routhian surface model, which includes a quadrupole-quadrupole pairing term [22]. These results indicate that a prolate shape is favored for  $^{72}\text{Kr}$  at low spin ( $\sim 6\hbar$ ). The calculations were able to reproduce the  $g_{9/2}$  proton and neutron crossing frequencies in both  $^{74,76}\text{Kr}$  [10,19]. However, they predict a crossing frequency of  $\sim 0.58$  MeV/ $\hbar$  for  $^{72}\text{Kr}$ , which is clearly much too low. This decrease in crossing frequency is due to the fact that the calculations predict a reduction in the quadrupole deformation, from  $\sim 0.38$  for the vacuum configuration to  $\sim 0.30$  for the aligned four quasiparticle configuration, as well as a shift from a near-prolate ( $\gamma \sim 5^\circ$ ) to a more triaxial ( $\gamma \sim -25^\circ$ ) nuclear shape. These results indicate that there are problems in describing the properties of  $^{72}\text{Kr}$  within the model.

Previous work [2,8,9] has demonstrated that the  $np$  interaction may cause a delay of the first band crossing in even  $N=Z$  nuclei as compared to the neighboring even-even isotopes. In order to study these features further, we have performed cranking calculations within an exactly solvable model of a deformed single- $j$  shell ( $g_{9/2}$ ). The Hamiltonian consists of a cranked deformed one body term and a scalar two-body delta interaction [23,24]. The model contains the deformation parameter  $\kappa$  and the strength of the delta interaction as the parameters. In our calculations we used  $\kappa = 2.4$ , which approximately corresponds to  $\beta = 0.4$ . For the strength of the delta interaction we used  $G = 1$  MeV, which is consistent with earlier calculations [25].

The results for  $^{72}\text{Kr}$  are shown in Fig. 5(a) and may be compared to the experimental data in Fig. 5(b). It should be noted that because of the limitations of the calculations only qualitative comparisons should be made with the data. In the  $N=Z$  case there is a double alignment predicted [24], i.e., the ground state band ( $g$  band) is crossed by the four quasiparticle band (double  $S$  band) with both a pair of  $g_{9/2}$  protons and neutrons aligned. In the  $N=Z+2$  nucleus,  $^{74}\text{Kr}$ , the first alignment results from a crossing with the single  $S$  band which contains only one pair of  $g_{9/2}$  nucleons. These features will be discussed further below.

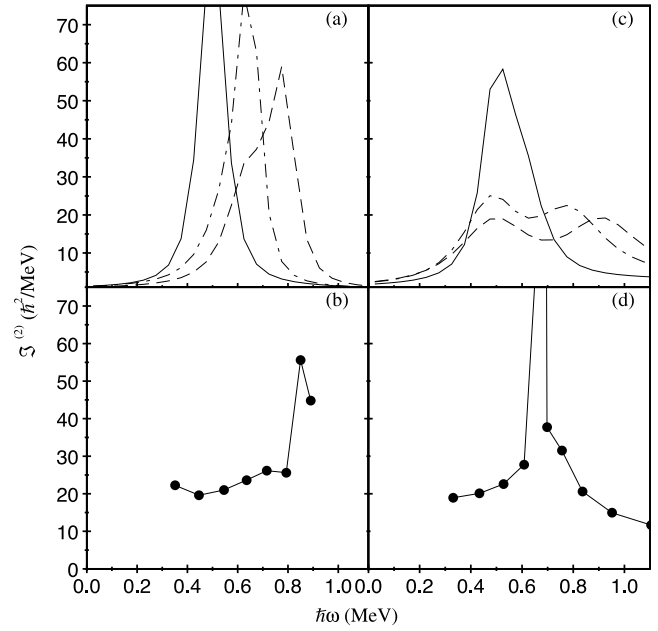


FIG. 5. The upper panels show the theoretical dynamic moment of inertia plots for (a)  $^{72}\text{Kr}$ , (c)  $^{74}\text{Kr}$ . The solid lines represent the results of the calculations with no  $np$  pairing, the dot-dashed lines correspond to the second set of calculations which involved both isovector and isoscalar  $np$  pairing but which had the  $T=0, J=1$  and  $T=0, J=9$  contributions set at similar strengths. The dashed line corresponds to the final set of calculations where both isovector and isoscalar  $np$  pairing were included but the  $T=0, J=1$  strength was increased by a factor of 2. The lower panels show the experimental dynamic moments of inertia plots for (b)  $^{72}\text{Kr}$  and (d)  $^{74}\text{Kr}$  for comparison.

In order to disentangle the effects of the  $np$  pairing we performed three sets of calculations. Initially, calculations were performed with the  $np$  part of the interaction switched off. These gave  $g_{9/2}$  proton and neutron crossing frequencies for  $^{72}\text{Kr}$  of  $\omega \sim 0.5$  MeV/ $\hbar$  [Fig. 5(a)], which are similar to the values obtained from standard CSM calculations (0.56 MeV/ $\hbar$ ). Similar calculations for  $^{74}\text{Kr}$  predict almost the same crossing frequency [Fig. 5(c)].

In the second set of calculations, the  $np$  correlations were taken into account by using the full delta interaction. As discussed in Ref. [2], the crossing frequency in the  $N=Z$  nucleus is considerably delayed relative to that in the  $N=Z+2$  nucleus. The calculated shift in the crossing frequency for the  $g_{9/2}$  protons and neutrons is clearly seen in Fig. 5(a), where for  $^{72}\text{Kr}$  it is shifted up to  $\sim 0.63$  MeV/ $\hbar$ . This delay in crossing frequency may be explained as follows. The  $T=1$   $np$  correlations lower the energy of the  $g$  band because the  $np$  pairs contribute to the correlation energy in addition to the  $pp$  and  $nn$  pairs. In the backband region pairs of  $g_{9/2}$  protons and neutrons align, consequently, they are blocked out of the  $T=1$  pair correlations since, for  $J=0$  pairs, the particles must be antialigned. Hence the gain in  $np$  correlation energy is reduced and the  $S$  band is shifted up in energy relative to the  $g$  band.

In the case of  $T=0$  pairing, the  $J=1$  and  $J=9$  components of the  $np$  interaction have a counteracting tendency.

The attractive  $J=9$  component favors the parallel orientation of the  $g_{9/2}$  proton spin with respect to the  $g_{9/2}$  neutron spin, i.e., it lowers the energy of the double  $S$  band which contains the four aligned  $g_{9/2}$  particles. On the other hand, the  $J=1$  component generates correlations which involve pairs of protons and neutrons with nearly antiparallel spins. Thus, like the  $J=0$  correlations, these correlations also raise the energy of the double  $S$  band with respect to the  $g$  band. It has been shown in Ref. [26] that for a delta interaction the total  $T=0$  pairing has no effect on the band crossings, because the  $T=0, J=1$  and  $T=0, J=9$  components, which individually change the crossing frequency, happen to cancel each other. Thus the calculated shift in the crossing frequency at this point may be attributed solely to the  $T=1$  component of the pure  $\delta$  force.

In a real nucleus one may expect that the  $T=0, J=1$  pairing dominates over the  $T=0, J=9$  pairing term since in a multiconfiguration space more  $j$  states will contribute to the  $T=0, J=1$  than to the  $T=0, J=9$  pairing. In order to model this effect we have increased the strength of the  $T=0, J=1$  component of the  $np$  force by a factor of 2. (This change makes minimal difference to the odd-even binding energies, the results remaining consistent with experimental values.) Figure 5(a) shows that in  $^{72}\text{Kr}$  this results in a further, significant, delay of the  $g_{9/2}$  proton and neutron crossing frequencies from 0.63 to  $\sim 0.8$  MeV/ $\hbar$ . These results indicate that the presence of both  $T=1$  and  $T=0$   $np$  pairing terms could explain the substantial increase in the crossing frequencies of the  $g_{9/2}$  protons and neutrons.

For  $^{74}\text{Kr}$  [Figs. 5(c) and 5(d)], the  $np$  correlations have the consequence that the four  $g_{9/2}$  particles align in two well-separated steps, which show up as the two humps in Fig. 4(c). The first maximum lies at about the same frequency as the calculations without the  $np$  correlations, however, the second is shifted to considerably higher frequency. Thus the double alignment in  $N=Z$  nuclei is delayed relative to the first single alignment in the  $Z=N+2$  nucleus. This is what seems to be observed for  $^{72,74}\text{Kr}$ . The experimental alignment ( $\sim 7.5\hbar$ ) at the band crossing in  $^{74}\text{Kr}$  suggests that only one pair of  $g_{9/2}$  particles is aligned, furthermore, the band crossing appears at a substantially lower frequency than the up bend in  $^{72}\text{Kr}$ . The predicted high frequency of the second alignment in the  $Z=N+2$  nucleus is consistent with the fact that no second crossing is seen in  $^{74}\text{Kr}$ . It is clear, however, that the observation of higher spin states in  $^{72}\text{Kr}$  will be essential in order to see if additional (i.e., a double) alignment is present in this case at  $\omega \sim 0.85$  MeV/ $\hbar$ . (Note that the extra transitions observed by Fischer and Lister [12] do not appear to be sufficient to resolve this issue.) Experimentally, the observed sharp first up bend in  $^{74}\text{Kr}$  [Fig. 5(d)] is clearly in disagreement with the present calculations, which predict a rather smooth alignment. However, the sharpness of the backbend is known to be sensitive to the details of the model used. In view of the qualitative character of the present model analysis, we do not consider this discrepancy to be a serious flaw.

Finally, one should note that there is experimental evidence for a substantial shape change after the  $S$ -band cross-

ing in the yrast band of  $^{74}\text{Kr}$  [27]. Moreover, the dynamic moments of inertia of the yrast bands of  $^{74-76}\text{Kr}$  also indicate that there is a shrinking of the deformation above the backbend. At the present time the available data for  $^{72}\text{Kr}$  suggest that this shrinking does not seem to be present, however, the  $^{74}\text{Kr}$  work reminds us that shape changes could play a very important role. It is also worth noting that the Excited Vampir calculations for  $^{72,74}\text{Kr}$  [20] suggest that there is substantial mixing of co-existing states based on prolate configurations having different quadrupole, hexadecapole and octupole deformations at high spins. Clearly, in order to take this work further it will be important to deduce both the deformation and shape of the nucleus in the band crossing region so that the precise effect of the shape changes on the  $g_{9/2}$  proton and neutron crossing frequencies can be determined, thereby allowing the  $np$  correlation effects to be better quantified.

## V. SUMMARY

In conclusion, we have observed the yrast band in  $^{72}\text{Kr}$  up to a tentative spin of  $20\hbar$  and established the presence of two new sideband structures. An alignment, which is thought to result from the crossing of the vacuum configuration with the four quasiparticle band containing aligned pairs of  $g_{9/2}$  neutrons and protons, is observed in the yrast band, and has been shown to be significantly delayed in frequency with respect to the heavier even-even Kr isotopes ( $^{74,76}\text{Kr}$ ). Calculations, performed within a deformed single- $j$  shell, suggest that this delayed band crossing may be attributable to the presence of both isovector ( $T=1$ ) and isoscalar ( $T=0$ )  $np$  pairing correlations. It must be borne in mind, however, that our shell model calculations do not distinguish between the particle-hole and the particle-particle channel, hence they only demonstrate that correlations between the protons and neutrons within the  $g_{9/2}$  shell may be responsible for the delay. The fact that these correlations are in the pairing (i.e., particle-particle) channel is likely, but not proven. It should also be noted that if  $^{72}\text{Kr}$  were to remain oblate at high spin rather than having a prolate deformation, as state of the art self-consistent cranking calculations suggest, and  $^{74,76}\text{Kr}$  were prolate, the presence of a strong  $np$  interaction would not be necessary to explain the observed data. An important aspect of future work will be the determination of the deformation of the nucleus in the band crossing region.

## ACKNOWLEDGMENTS

The authors would like to thank the staff at the ATLAS accelerator for providing the beam and John Greene for manufacturing the targets. This work was supported by the U.K. EPSRC, U.S. NSF, and U.S. Department of Energy under Contract Nos. DE-AC03-76SF00098, DE-FG02-95ER40934, and W-31-109-ENG38. R.M.C. and R.W. also wish to acknowledge support from NATO.

- [1] A. L. Goodman, *Adv. Nucl. Phys.* **11**, 263 (1979).
- [2] S. G. Frauendorf and J. A. Sheikh, *Phys. Rev. C* **59**, 1400 (1999).
- [3] W. Satula and R. Wyss, *Phys. Lett. B* **393**, 1 (1997).
- [4] A. O. Macchiavelli *et al.*, *Phys. Rev. C* **61**, 041303(R) (2000).
- [5] P. Vogel, *Nucl. Phys.* **A662**, 148 (2000).
- [6] D. R. Bes, R. A. Broglia, O. Hansen, and O. Nathan, *Phys. Rep.*, *Phys. Lett.* **34C**, 1 (1977).
- [7] A. O. Macchiavelli *et al.*, *Phys. Lett. B* **480**, 1 (2000).
- [8] K. Kaneko and J-Y. Zhang, *Phys. Rev. C* **57**, 1732 (1998).
- [9] J. A. Sheikh and R. Wyss, *Phys. Rev. C* **62**, 051302(R) (2000).
- [10] G. de Angelis *et al.*, *Phys. Lett. B* **415**, 217 (1997).
- [11] P. Hausladen, Ph.D. thesis, University of Pennsylvania, 1998.
- [12] S. M. Fischer *et al.*, Nuclear Structure 2000 Conference, MSU, MI 48824 USA [*Nucl. Phys. A* (to be published)]; C. J. Lister, PINGST 2000 Conference Lund (see <http://pingst2000.kosufy.lu.se/proceedings.asp>).
- [13] I. Y. Lee, *Nucl. Phys.* **A520**, 641c (1990).
- [14] D. G. Sarantites, P. F. Hua, M. Delvin, L. G. Sobotka, J. Elson, J. T. Hood, D. R. LaFosse, J. E. Sarantites, and M. R. Maier, *Nucl. Instrum. Methods Phys. Res. A* **381**, 418 (1996).
- [15] D. G. Sarantites (unpublished).
- [16] D. Seweryniak, J. Nyberg, C. Fahlander, and A. Johnson, *Nucl. Instrum. Methods Phys. Res. A* **340**, 353 (1994).
- [17] D. C. Radford, *Nucl. Instrum. Methods Phys. Res. A* **361**, 297 (1995).
- [18] K. S. Krane, R. M. Steffen, and R. M. Wheeler, *Nucl. Data Tables* **11**, 351 (1973).
- [19] D. Rudolf *et al.*, *Phys. Rev. C* **56**, 98 (1997).
- [20] A. Petrovici, K. W. Schmid, and A. Faessler, *Nucl. Phys.* **A665**, 333 (2000).
- [21] R. Bengtsson and S. Frauendorf, *Nucl. Phys.* **A327**, 139 (1979).
- [22] W. Satula and R. Wyss, *Phys. Scr.* **T56**, 159 (1995).
- [23] J. A. Sheikh, P. Van Isacker, D. D. Warner, and J. A. Cameron, *Phys. Lett. B* **252**, 314 (1990).
- [24] J. A. Sheikh, N. Rowley, M. A. Nagarajan, and H. G. Price, *Phys. Rev. Lett.* **64**, 376 (1990).
- [25] D. Rudolf *et al.*, *Phys. Rev. Lett.* **76**, 376 (1996).
- [26] S. G. Frauendorf and J. A. Sheikh, *Nucl. Phys.* **A645**, 509 (1999).
- [27] A. Algora *et al.*, *Phys. Rev. C* **61**, 031303(R) (2000).